THE JOURNAL OF PHYSICAL CHEMISTRY A LETTERS

2006, *110,* 3853−3856
Published on Web 02/25/2006

Evidence for the Production of N_4 via the N_2 $A^3\Sigma_u^+$ + N_2 $A^3\Sigma_u^+$ Energy Pooling Reaction

Jeffrey Barber,† Douglas E. Hof, Chad A. Meserole, and David J. Funk*

Dynamic Experimentation Division, Los Alamos National Laboratory, Los Alamos, New Mexico 87545

Received: January 29, 2006; In Final Form: February 14, 2006

We report mass spectrometric evidence supporting our proposed mechanistic pathway for the production of N_4 through the energy pooling reaction N_2 $A^3\Sigma_u^+$ + N_2 $A^3\Sigma_u^+$. N_2 $A^3\Sigma_u^+$ is generated from the quenching of resonantly excited xenon in a mixture of xenon, $^{15}N_2$, and $^{14}N_2$ that is illuminated with xenon resonant lamps (147 nm). Mass spectra are periodically taken of the mixture. Over time, we observe significant isotopic scrambling of the $^{15}N_2$ and $^{14}N_2$, generating $^{15}N^{14}N$ in concentrations approaching 10% (∼2 Torr) of the initial $^{15}N_2$ concentration. Though we do not observe the direct formation of N_4, the isotopic ratios indicate that an excited complex ($^{15}N_2{}^{14}N_2$) exists long enough so that scrambling of the nitrogen atoms can occur, offering a possible route to the formation of tetrahedral nitrogen (^1T_d N_4).

Introduction

Tetrahedral nitrogen (tetraazatetrahedrane, N_4 ^1T_d), was first predicted as a stable isomer of nitrogen in the early 1970s.[1] Since that time, a number of theoretical calculations have been performed at increasing levels of sophistication that have supported these first calculations.[2] Interest in the experimental confirmation of these calculations increased over the years, culminating with the funding of programs to pursue the synthesis of N_4 as well as other allotropes of nitrogen. The interest lies in the fact that all of the predicted allotropes of nitrogen are energetic and would form the basis for a new set of environmentally friendly, or "green", energetic materials. At that time, we proposed a concept of photosensitization of N_2 for the production of N_4, analogous to mercury photosensitization of hydrocarbons.[3] Early on, it became clear that a simple scheme, such as

$$N_2\ X^1\Sigma_g^+ + M^*\ (M = Kr, Xe) \rightarrow N_2^*\ (\text{state not specified})$$

$$N_2^* + N_2\ X^1\Sigma_g^+ + M \rightarrow {}^1T_d\ N_4 + M \qquad (1)$$

is not, practically speaking, feasible, given the known energetics and orbital diagrams of these species. However, in the 1995 paper by Dunn and Morokuma,[4] it was shown that the long-range N_2 fragments correlated (at large molecular separation) with *both* fragments electronically excited, each having an electronic configuration of $\pi^3\pi^{*1}$. A review of the comprehensive spectroscopic data set of N_2 revealed that the lowest excited state to contain the required symmetry is the $A^3\Sigma_u^+$ state of N_2,[5] which, coincidentally, has a 1.9 s fluorescence lifetime, with this exceptionally long lifetime critical to our proposed mechanism for the formation of N_4 (M is a third body):

$$N_2\ A^3\Sigma_u^+ + N_2\ A^3\Sigma_u^+ + M \rightarrow N_4\ {}^1T_d + M \qquad (2)$$

Reaction 2 is a possible singlet-coupled channel of the well-known energy pooling reaction of N_2 $A^3\Sigma_u^+$ + N_2 $A^3\Sigma_u^+$, first observed by Stedman and Setser in 1969[6] and later by Hays and Oksam in 1973.[7] The detailed study of this reaction has provided rate constants and hence "branching" ratios for the energy pooling of the A-state as follows:[8−10]

$$N_2\ A^3\Sigma_u^+ + N_2\ A^3\Sigma_u^+ \rightleftharpoons N_2\ B\ {}^3\Pi_g \qquad k \sim 1 \times 10^{-10}\ \text{cm}^3/\text{molecule/s} \quad (3)$$

$$N_2\ A^3\Sigma_u^+ + N_2\ A^3\Sigma_u^+ \rightleftharpoons N_2\ C\ {}^3\Pi_u \qquad k \sim 1.5 \times 10^{-10}\ \text{cm}^3/\text{molecule/s} \quad (4)$$

$$N_2\ A^3\Sigma_u^+ + N_2\ A^3\Sigma_u^+ \rightleftharpoons N_2\ C'\ {}^5\Pi \qquad k \sim 2.5 \times 10^{-11}\ \text{cm}^3/\text{molecule/s} \quad (5)$$

$$N_2\ A^3\Sigma_u^+ + N_2\ A^3\Sigma_u^+ \rightleftharpoons N_2\ C''\ {}^5\Pi \qquad k \sim 9 \times 10^{-11}\ \text{cm}^3/\text{molecule/s} \quad (6)$$

We note that reaction of two molecules, each triplet coupled, will lead to potential surfaces that are singlet, triplet, and quintuplet coupled. As identified in reactions 3−6, the triplet and quintuplet branches are open and available for the energy pooling reactions. However, the singlet channel has never been observed. The absence of the observation of a singlet channel may result from (a) no reaction, (b) a dark channel leading to the production of ground state nitrogen molecules, or (c) a dark channel producing highly excited N_4 (excess energy of ∼20 000 cm^{-1}; ∼36 500 cm^{-1} above the ground rovibrational state of N_4) that would dissociate in the absence of quenching collisions. Thus, the singlet coupled surface may provide a pathway for generating singlet N_4 (highly vibrationally excited: either tetrahedral[4] or rectangular[11]) that eventually could be quenched to ground-state N_4.

* Corresponding author. E-mail: djf@lanl.gov.
† Current address: Battelle Memorial Institute, William J. Hughes Technical Center, Transportation Security Laboratory, Atlantic City International Airport, NJ 08405.

10.1021/jp060616w CCC: $33.50

To attempt a practical realization of our scheme, we used known quenching pathways, which allowed us to develop the following mechanism and energy flow system:[12]

$$\mathrm{Xe} + h\nu\ (147\ \mathrm{nm}) \rightarrow \mathrm{Xe}\ [3/2]_1 \quad (7)$$

$$\mathrm{Xe}\ [3/2]_1 + \mathrm{N_2}\ X\,^1\Sigma_g^+ \rightarrow \mathrm{Xe} + \mathrm{N_2}\ B\,^3\Pi_g \quad (8)$$

$$\mathrm{N_2}\ B\,^3\Pi_g \rightarrow \mathrm{N_2}\ A\,^3\Sigma_u^+ + h\nu \quad (9)$$

$$^{15}\mathrm{N_2}\ A\,^3\Sigma_u^+ + {}^{14}\mathrm{N_2}\ A\,^3\Sigma_u^+ \rightarrow {}^{15}\mathrm{N_2}{}^{14}\mathrm{N_2} \rightarrow {}^{15}\mathrm{N_2} + {}^{14}\mathrm{N_2}\ \text{or}\ 2\ {}^{15}\mathrm{N}{}^{14}\mathrm{N} \quad (10)$$

where reaction 10 is assumed to occur in the absence of quenching collisions. Thus, if the A-state of nitrogen could be made in high enough concentration (which is feasible given the 1.9 s lifetime), reactions 3−6 and 10 could occur with good efficiency. A more detailed kinetic scheme using all of the known kinetic parameters and fluorescent lifetimes available in the literature, and a rate constant for N_4 creation equivalent to those measured by Piper for the triplet and quintuplet channels, was used to determine an approximate optimal nitrogen pressure for this reaction.[13] This optimal pressure is less than 50 Torr and results from the fact that the B-state in reaction 8 can be depleted through self-quenching by ground-state nitrogen as identified by Piper.[9] Thus, by illuminating a mixture of xenon, $^{15}N_2$, and $^{14}N_2$ with xenon resonance radiation, we expect to see scrambling of the isotopes if the excited-state intermediate of reaction 10 results in either a single bonded nitrogen structure (tetrahedral N_4) or through a double bonded resonance structure (via rectangular N_4)[11] *and* lives long enough for the atoms to lose memory of their initial atomic partner.

Other groups have proposed alternative schemes and have conducted experiments in an attempt to form N_4. Ostmark and co-workers have proposed a mechanism similar to reaction 1: the difference is that the excited N_4 would be generated through excitation of nitrogen using laser radiation, ion bombardment, or in hollow cathode discharge.[14] They have not observed the formation of N_4 to date. Radziszewski and co-workers have conducted a number of experiments in which a microwave discharge of pure nitrogen is generated and the resulting fragments and species are collected on a helium cooled sapphire window.[15] The resulting nitrogen "ice" gave rise to the observation of a weak peak at the expected N_4 IR active frequency of ~936 cm^{-1}. However, substitution to the $^{15}N_2$ starting material led to an isotopic shift that was inconsistent with that expected for this molecule.[16] Finally, Cacace et al. have observed an N_4^+ cation in a neutralization-reionization experiment that they have attributed to the weakly bound open chain form of N_4.[17]

Experimental Section

A mixture of 2 Torr Xe (Air Products 99.995%), 20 Torr $^{15}N_2$ (Cambridge Isotopes, 98%), and 20 Torr "standard" N_2 (UHP 99.999%; 99.635% ^{14}N) was prepared in a small vacuum chamber consisting of a double-sided $2^3/_4$ in. knife-edge flange (MDC vacuum) mated to two double-sided knife-edge flange LiF windows (St. Gobain), as shown in Figure 1. The gases were additionally purified to below ppb impurity levels by passage through SAES PS11 series ambient temperature gas purifiers before mixing in the cell. Xenon resonance lamps (10:1, 147 nm:129.5 nm; COREX of Russia; ~20 mW average power) were mounted in water-cooled stainless nipples, which were back-filled with UHP argon (620 Torr 99.999%) and bolted to the LiF window flanges. The VUV radiation passed through LiF windows into the ~30 cm^3 volume cell. Mass spectra were taken periodically over several weeks using a Ominstar GSD 300 (Pfeiffer Vacuum). Calibration and normalization was accomplished by scaling the mass spectral intensities to maintain a constant xenon signal, which should not change over time. Two replica experiments were performed to demonstrate reproducibility.

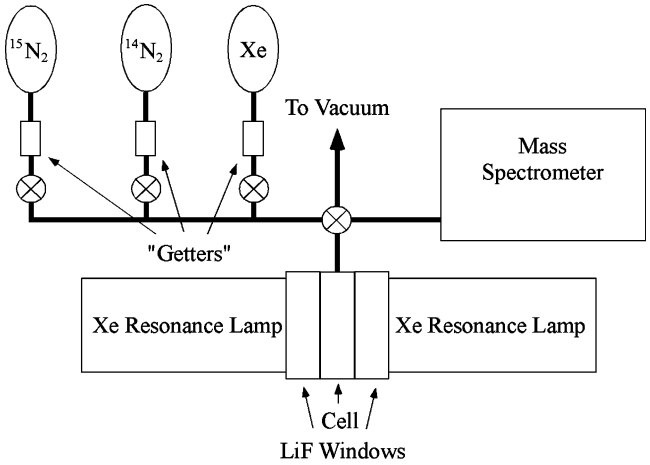

Figure 1. Schematic of the experimental apparatus.

Results

The Xe signal in the mass spectra is used for an internal standard, and all mass spectra are Xe peak area normalized such that the area under the curve from 126 *m*/*z* to 137 *m*/*z* is equal to 1. Prior to normalization, a simple baseline correction is performed using the best fit line through a highly linear region of the spectra from 50 *m*/*z* to 60 *m*/*z* and from 70 *m*/*z* to 120 *m*/*z* (Xe^{+2} peaks are omitted) and this line is subtracted from each spectrum. Without this baseline correction, the peak area of the Xe species would be overestimated by as much as 1.2%. Following the baseline correction and peak area normalization, the peaks (or clusters of peaks) of interest are fit with commercially available software (PeakFit) to separate overlapping peaks, e.g., 28, 29, and 30 *m*/*z*.

Baseline-corrected, Xe^+-normalized mass spectra are illustrated in Figure 2 for the range 24−34 *m*/*z*. This series of spectra shows the time evolution throughout the first experiment. From $t = 0$ days to $t = 24$ days, there is a clear increase in the 29 *m*/*z* peak ($^{14}N^{15}N$). During this time period, the reaction cell is illuminated with the lamps. After the 24th day, the lamps are switched off. While the lamps are switched off, there is no appreciable change to the 29 *m*/*z* signal. Given that the 29 *m*/*z* peak increases under VUV irradiation and remains constant under conditions of no illumination suggest that isotope exchange only takes place (to any measurable extent) when the reaction is provided energy via the VUV photons and that, once exchanged, the $^{14}N^{15}N$ molecules are stable in the absence of VUV, as to be expected. These two observations provide strong evidence that our proposed reaction mechanism may be correct and could form the basis for N_4 synthesis. The *increase* in 29 *m*/*z* peak and simultaneous *decrease* in 30 *m*/*z* peak seen in our mass spectra indicate that an excited complex of N_4 with the proper bonding and sufficient lifetime to allow for this exchange to occur. Shown in Figure 3 are the time-dependent mass spectra for the second experimental run, demonstrating both reproducibility and an increase in the 29 *m*/*z* peak to ~10% of the 30 *m*/*z* peak.

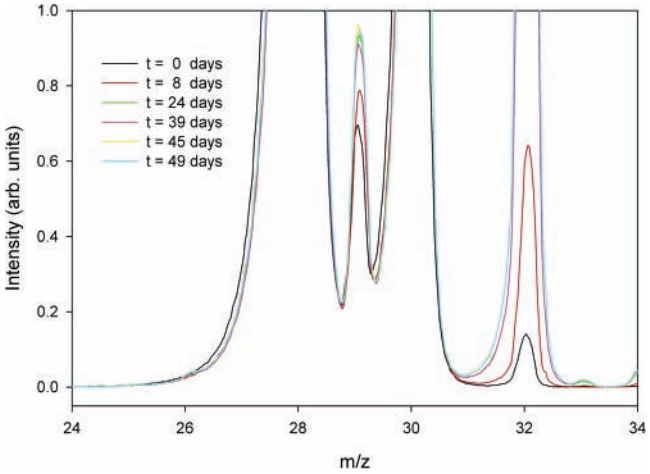

Figure 2. Mass spectra from 24 *m*/*z* to 34 *m*/*z* over the course of 49 days. The VUV lamps are illuminating the cell for the first 24 days only. During this period, there is a significant increase of the 29 *m*/*z* peak. After the lamps are switched off, the change of the 29 *m*/*z* peak is insignificant.

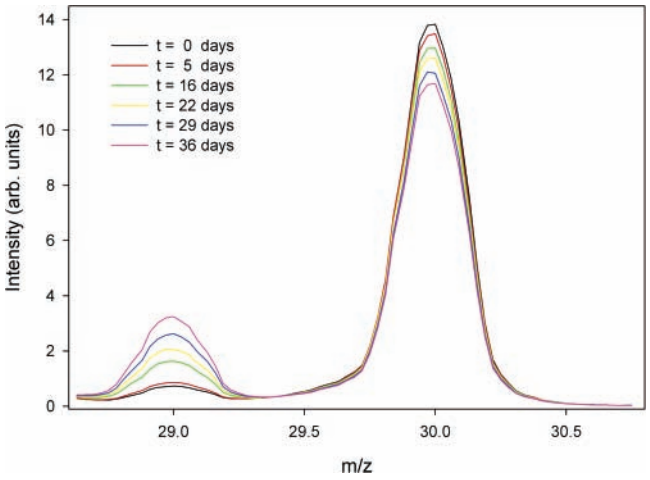

Figure 3. Mass spectra from 28.6 *m*/*z* to 30.75 *m*/*z* over the course of 36 days. The VUV lamps are illuminating the cell for the entire time. During this period, there is a significant increase of the 29 *m*/*z* peak, with a corresponding decrease in the 30 *m*/*z* peak.

Because the peak at 29 *m*/*z* is expected to be a reaction product of atom exchange between $^{14}N_2$ (28 *m*/*z*) and $^{15}N_2$ (30 *m*/*z*), tracking the temporal evolution of these and other species provide clues as to what is taking place in the reaction cell with the lamps on and off. The relative peak areas for peaks at 18, 28, 29, 30, 32, and 44 *m*/*z* are plotted in Figure 4. During the portion of the experiment when the reaction cell is irradiated with VUV, there is a dramatic increase in the 29 *m*/*z* peak and a concomitant decrease in the 28 *m*/*z* and 30 *m*/*z* peaks. The decrease in these two peaks is not unexpected, as the gain of $^{14}N^{15}N$ must come with the loss of both $^{14}N_2$ and $^{15}N_2$. During the period of no illumination, the peak at 30 *m*/*z*, much like the peak at 29 *m*/*z*, remains relatively constant. There is, however, an increasing trend in the 28 *m*/*z* peak. There are several possible explanations. First, $^{12}C^{16}O$ and $^{14}N_2$ are isobaric interferences and any $^{12}C^{16}O$ in the system will appear as $^{14}N_2$. The CO may arise as a decomposition product of CO_2, due to reactions taking place either in the reaction cell or during the ionization and detection event in the mass spectrometer. Additionally, the reaction cell is not actively pumped once it is filled with the reactant gases to a total pressure far less than atmospheric pressure. Therefore, it is possible that N_2, CO, and CO_2 are leaking into the cell.

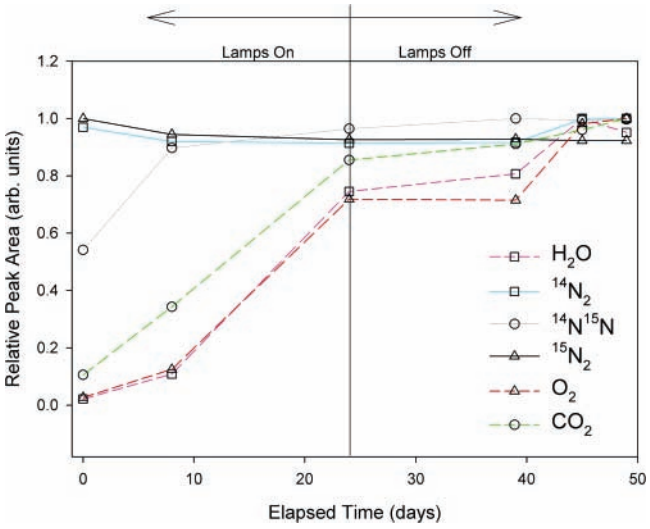

Figure 4. Relative mass spectra peak areas as a function of time. Several peaks in the mass spectra are tracked as a function of time to understand what is taking place in the reaction cell. Peaks for $^{14}N_2$ (28 *m*/*z*) [solid line, squares], for $^{14}N^{15}N$ (29 *m*/*z*) [solid line, circles], and for $^{15}N_2$ (30 *m*/*z*) [solid line, triangles] are directly related to the isotope exchange reaction. Peaks for H_2O (18 *m*/*z*) [dashed line, squares], for O_2 (32 *m*/*z*) [dashed line, triangles], and for CO_2 (44 *m*/*z*) [dashed line, circles] are indicators of an atmospheric leak into the cell or are indicators of unintentional reactions.

Evidence for atmospheric contaminants leaking into the cell is provided by tracking the evolution of the peaks at 18 *m*/*z* (H_2O), at 32 *m*/*z* (O_2), and at 44 *m*/*z* (CO_2). All these tend to increase as time is elapsed. The rate of increase is most dramatic while the lamps are illuminating the reaction cell but continue to increase after the lamps are switched off. Two likely explanations are (1) the heat from the lamps stresses the flanges, making a leak more probable and (2) the VUV is stimulating the desorption of $C_xO_yH_z$ species directly (or indirectly with H_2O, CO, and CO_2 as major decomposition products) from the stainless steel vacuum walls.

Despite the certain interference at 28 *m*/*z*, the peaks at 29 *m*/*z* and at 30 *m*/*z* are not appreciably affected by the leak and or stimulated desorption, because of the extremely low isotopic abundances of ^{13}C (1.07%), of ^{17}O (0.038%), and of ^{18}O (0.205%). The contributions of $^{13}C^{16}O$ and of $^{12}C^{17}O$ to 29 *m*/*z* are negligible. Likewise, the contribution of $^{13}C^{17}O$ to 30 *m*/*z* is insignificant. Therefore, the 29 *m*/*z* and 30 *m*/*z* peaks are better indicators of the reaction progress due to the smaller contributions from interferences. In fact, the 30 *m*/*z* peak behaves as expected on the basis of the behavior of the 29 *m*/*z* peak. The 30 *m*/*z* peak decreases while the lamps are on with the concomitant increase in the 29 *m*/*z* peak, and while the lamps are off, the 30 *m*/*z* peak remains largely unchanged, just as the 29 *m*/*z* peak.

Conclusion

Here, we present results of our ongoing efforts to synthesize tetrahedral nitrogen, N_4. Mass spectrometric observations show that resonant energy transfer from Xe* to N_2 has allowed for isotopic exchange to occur between $^{14}N_2$ and $^{15}N_2$, creating the mixed-isotopic species $^{14}N^{15}N$. Although N_4 has yet to be observed directly, this is a promising development due to the inherent stability in the nitrogen−nitrogen triple bond. The increase in 29 *m*/*z* peak and simultaneous decrease in 30 *m*/*z* peak seen in our mass spectra indicate the existence of an excited complex of N_4 with the proper bonding and sufficient lifetime

to allow for this exchange to occur. We note that an alternate possibility exists, which is that the energy pooling reaction leads to dissociation of either the $^{14}N_2$ and $^{15}N_2$, yielding atomic nitrogen that subsequently recombines forming $^{14}N^{15}N$. We believe that this is unlikely, because the excitation energy from both molecules must end up in one molecule to yield dissociation, which seems improbable given the known orbital relationships (see ref 11). Experiments are underway in an effort to quench some portion of the N_4 complex to either the theoretically stable tetrahedral or rectangular species.

Acknowledgment. This research was conducted at Los Alamos National Laboratory under contract W-7405-ENG-36, with support from DARPA and the Agnew National Security Postdoctoral Program at Los Alamos. C.A. Meserole would like to acknowledge the assistance of Greg Fisher in critical discussions and review of this manuscript.

References and Notes

(1) Guest, M. F.; Hillier, I. H.; Saunders: V. R. *J. Chem. Soc., Faraday Trans. 2* **1972**, *68*, 2070.

(2) See for example, Glukhovtsev, M. N.; Laiter, S. *J Phys. Chem.* **1996**, *100*, 1569−1577 and references therein.

(3) Okabe, H. *Photochemistry of Small Molecules*; Wiley: New York, 1978.

(4) Dunn, K. M.; Morokuma, K. *J. Chem. Phys.* **1995**, *102*, 4904.

(5) Lofthus, A.; Krupenie, P. H. *J. Phys. Chem. Ref. Data* **1977**, *6*, 113−307.

(6) Stedman, D. H.; Setser, D. W. *J. Chem. Phys.* **1969**, *50*, 2256−58.

(7) Hays, G. N.; Oskam, H. J. *J. Chem. Phys.* **1973**, *59*, *11*, 6088−91.

(8) Piper, LG *J. Chem. Phys.* **1988**, *88*, 231−9.

(9) Piper, LG *J. Chem. Phys.* **1988**, *88*, 6911−21.

(10) Simek, M. *Plasma Sources Sci. Technol.* **2003**, *12*, 421−431.

(11) Bickelhaupt, F. M.; Hoffman, R.; Levine, R. D. *J. Phys. Chem.* **1997**, *101*, 8255−8263.

(12) See for example, Aquilanti, V.; Candori, R.; Pirani, F.; Ottinger, C. *Chem. Phys.* **1994**, *187*, 171−83 and references therein.

(13) Funk, D. J.; Barber, J. Unpublished results.

(14) Ostmark, H.; Launila, O.; Wallin, S.; Tryman, R. *J. Raman Spectrosc.* **2001**, *32*, 195−199.

(15) Zheng, J. P.; Waluk, J.; Spanget-Larsen, J.; Blake, D. M.; Radziszewski, J. G. *Chem. Phys. Lett.* **2000**, *328*, 227−33.

(16) Lee, T. J.; Martin, J. M. L. *Chem. Phys. Lett.* **2002**, *357*, 319−25.

(17) Cacace, F.; de Petris, G.; Troiani, A. *Science* **2002**, *295*, 480−81.